



Pressure-induced superconductivity and large upper critical field in the noncentrosymmetric antiferromagnet CeIrGe₃

F. Honda,¹ I. Bonalde,^{2,3} K. Shimizu,² S. Yoshiuchi,¹ Y. Hirose,¹ T. Nakamura,¹ R. Settai,¹ and Y. Ōnuki¹

¹Graduate School of Science, Osaka University, Toyonaka, Osaka 560-0043, Japan

²KYOKUGEN, Center for Quantum Science and Technology under Extreme Conditions, Osaka University, Toyonaka, Osaka 560-8531, Japan

³Centro de Física, Instituto Venezolano de Investigaciones Científicas, Apartado 20632, Caracas 1020-A, Venezuela

(Received 6 January 2010; revised manuscript received 20 February 2010; published 22 April 2010)

We report on the discovery of superconductivity in the noncentrosymmetric antiferromagnet CeIrGe₃ below 1.5 K at a pressure of 20 GPa. We performed electrical resistivity measurements in single crystals of CeIrGe₃ in the temperature range 0.04–300 K at pressures up to 24 GPa. From these measurements we deduced the P - T phase diagram. The data imply a crossover from localized to itinerant $4f$ electrons of the type caused by a Kondo-lattice phenomenon as pressure increases. The antiferromagnetic phase weakens with pressure and eventually vanishes above 22 GPa, indicative of the occurrence of a quantum critical point. Superconductivity appears inside the antiferromagnetic phase near this critical point. After the disappearance of the magnetic ordering a non-Fermi-liquid behavior is observed. Resistivity measurements taken at 24 GPa in magnetic fields up to 8 T strongly suggest that CeIrGe₃ has a very large upper critical field for $H_{\parallel}[001]$.

DOI: [10.1103/PhysRevB.81.140507](https://doi.org/10.1103/PhysRevB.81.140507)

PACS number(s): 74.70.Dd, 71.27.+a, 74.20.Rp, 74.62.Fj

Recently, the interplay of magnetism and superconductivity has attracted great interest with the discovery of several compounds in which a superconducting phase appears at the border of a magnetic order.^{1,2} These materials provide an important route to the understanding of superconductivity mediated by spin fluctuations associated with a magnetic quantum critical point (QCP). In most cases, these novel superconductors are based on either cerium or uranium. Of particular relevance is the influence of antiferromagnetism and superconductivity on each other in the cerium compounds that under pressure lose their antiferromagnetic (AFM) ordering at a critical pressure around which emerges the superconducting state. This phenomenology has become one of the most interesting issues in strongly correlated electron systems.

CeIrSi₃,³ CeRhSi₃,⁴ and CeCoGe₃ (Refs. 5 and 6) are among the Ce compounds showing superconductivity near a magnetic quantum phase transition. They belong to the series CeTX₃ (T =transition metal and X =Si, Ge) that crystallizes in the tetragonal BaNiSn₃-type structure *without* inversion symmetry. Thus, they are also part of the important class of novel superconductors that lack inversion symmetry. The absence of this symmetry causes the indistinguishability of the spin-singlet and spin-triplet states and the splitting of the parity-conserving spin degenerate energy bands. Due to this it is expected to see new phenomena in these superconductors.⁷ Some of the new behaviors indeed observed in CeIrSi₃, CeRhSi₃, and CeCoGe₃ are related to the upper critical field $H_{c2}(T)$: extremely large $H_{c2}^{\parallel}(0)$ s ($H_{\parallel}[001]$) compared to the critical temperatures, large anisotropies $H_{c2}^{\parallel}(0)/H_{c2}^{\perp}(0)$, and anomalous concave curvatures in $H_{c2}^{\parallel}(T)$.^{8,9}

CeNiGe₃, another member of the CeTX₃ family but that crystallizes in the orthorhombic SmNiGe₃-type structure *with* inversion symmetry, has a QCP and a superconducting phase appearing around this point.¹⁰ Interestingly, however, CeNiGe₃ has neither a high $H_{c2}(0)$ nor a $H_{c2}^{\perp}(T)$ with a concave curvature. Moreover, until now none unconventional

behavior has been observed in this compound. Thus, the lack of inversion symmetry seems to play a crucial role for the appearance of the unusual superconducting properties of CeIrSi₃, CeRhSi₃, and CeCoGe₃. The search for new noncentrosymmetric superconductors with quantum criticality is then of high interest. Here we report on the discovery of superconductivity near a QCP in the noncentrosymmetric compound CeIrGe₃. Previous works on CeIrGe₃ up to 8 GPa indicate the presence of antiferromagnetic phases at 4.7 and 8 K.^{11–13} The low- T phase shows weak ferromagnetic behavior at ambient pressure,¹¹ possibly due to canting of the magnetic moment with the Dzyaloshinskii-Moriya interaction and merges to the high- T phase around 4 GPa.¹² In the present work we found a QCP around 24 GPa and superconductivity about 20 GPa and below 1.5 K. Our results also point to a very high $H_{c2}(0)$ in CeIrGe₃, as is seen in CeIrSi₃, CeRhSi₃, and CeCoGe₃. To our knowledge, the superconducting critical pressure of 20 GPa in CeIrGe₃ is by far the highest in noncentrosymmetric and in heavy-fermion superconductors.

To eliminate the possibility of having traces of Bi in the resulting crystals, as occurred in CeCoGe₃,⁶ our single crystals of CeIrGe₃ were grown by the Sn-flux method. The crystals were grown by arc melting the proper amount of Ce (3N), Ir (4N), and Ge (5N). The samples were then placed along with Sn, in a composition of 1:20, in an alumina crucible that was maintained in a sealed quartz tube at 1000 °C for 2 days. After this, the quartz tube was cooled down quickly to 800 °C, then slowly (1 °C/h) to 600 °C and finally rapidly to room temperature. The excess of Sn was removed by spinning the ampoule in a centrifuge. The crystals grown by this procedure display the same thermodynamic, transport, and magnetic properties as those grown by the Bi-flux technique.^{12,13} Single crystal x-ray diffraction measurement was performed using a diffractometer with graphite monochromated Mo $K\alpha$ radiation. No second impurity phases were observed. The inset to Fig. 1(a) shows a

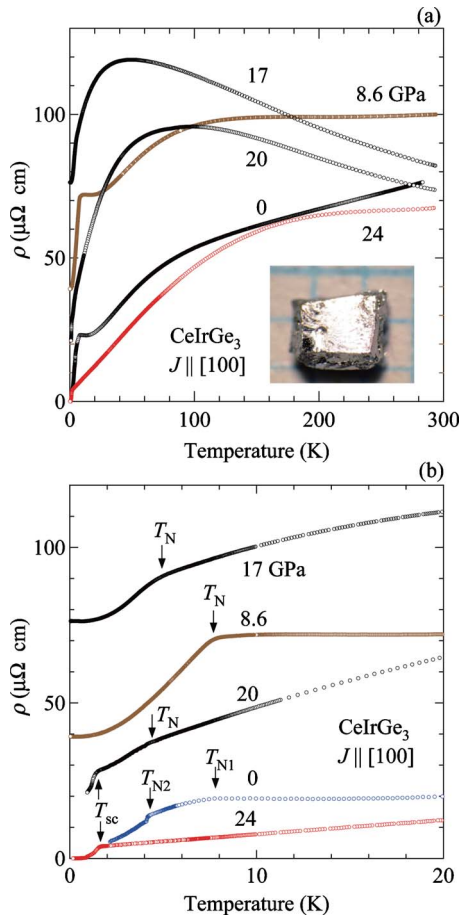


FIG. 1. (Color online) Electrical resistivity of CeIrGe_3 as a function of temperature at several pressures in the range 0–24 GPa (a) below room temperature and (b) below 20 K. The inset to (a) shows a picture of a CeIrGe_3 single crystal.

single crystal of CeIrGe_3 in which the flat plane is perpendicular to the c axis. Four-probe electrical resistivity measurements were performed with an LR-700 ac resistance bridge operating at 16 Hz. Temperatures as low as 40 mK were obtained with a dilution refrigerator. Pressures up to 24 GPa were applied with a CuBe-made diamond-anvil cell and were measured by the shift of the ruby R1 fluorescence line at room temperature. The pressure value was verified once at 40 K. NaCl powder was used as the pressure-transmitting medium. We were unable to carry out either ac susceptibility or specific-heat measurements because of the required high-pressure conditions.

Figure 1(a) shows the temperature dependence of the electrical resistivity of CeIrGe_3 for the sensing current along the [100] direction and for different pressures in the range 0–24 GPa. At low pressures the resistivity decreases with temperature and shows the appearance of AFM ordering at low temperatures, which is the usual behavior originated from localized $4f$ electrons. As pressure increases, the resistivity gradually develops a maximum around 100 K, from which it rapidly drops as temperature decreases, and ultimately shows a metallic response with no indication of AFM ordering. This implies a smooth change from localized $4f$ electrons at high temperatures to itinerant $4f$ electrons with

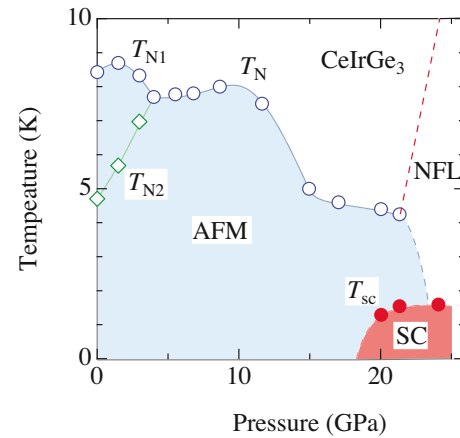


FIG. 2. (Color online) Phase diagram of CeIrGe_3 .

formation of heavy masses at low temperatures. Such a behavior provides a clear example of the crossover from localized to itinerant states caused by the Kondo-lattice phenomenon, as seen in CeCu_2Si_2 (Ref. 14) and CeCu_2Ge_2 .¹⁵ Notably, the temperature dependence of the resistivity of CeIrGe_3 below 300 K at different pressures differs from that of the sibling compounds CeIrSi_3 , CeRhSi_3 , and CeCoGe_3 , though it looks qualitatively similar to the one of CeNiGe_3 with inversion symmetry.¹⁰

Figure 1(b) displays the resistivity in the low-temperature region. It is observed that superconductivity occurs at 20 GPa, whereas AFM order fades away above 22 GPa. The resistivity at 24 GPa follows a T linear response above the superconducting transition in the temperature range 1.7–70 K, indicating that the system becomes a non-Fermi liquid. This behavior is found in the other four CeTX_3 superconductors as well. Superconductivity initially appears at 20 GPa as a drop in the resistivity to a nonzero value at the lowest temperatures. At 20 and 22 GPa extrapolations of the resistivity below T_c to $T=0$ K yield finite values. Superconductivity with zero resistivity is observed at 24 GPa. Pressure-induced superconductivity with nonzero resistivity in the low-pressure region has been also found in other heavy fermions, such as CeNiGe_3 (Ref. 10) and CeCoGe_3 ,⁵ and interestingly in the oxypnictide LaFeAsO .¹⁶ In all these materials superconductivity develops at relatively high pressures, which has led to the argument that the lack of zero resistivity could be due to defects or inhomogeneities created in the samples by the application of inherent nonuniform pressures. However, in CeCoGe_3 the resistivity sharply drops to zero only once the optimal pressure P_{opt} , at which the superconducting critical temperature has its maximum, has been applied.⁵ Here a similar compartment of the resistivity is observed in CeIrGe_3 .

In a previous report,¹² the pressure-temperature phase diagram of CeIrGe_3 was drawn up to 8 GPa with the sole existence of magnetic phases. Here we present in Fig. 2 an almost complete phase diagram up to 24 GPa in which the AFM transition temperature T_N falls to zero in two steps, the first around 10 GPa and the second about 21 GPa, and superconductivity appears at 20 GPa below 1.5 K. The quantum critical point ($T_N \rightarrow 0$) is somewhere near 24 GPa, thus the superconducting state emerges at a pressure at which the

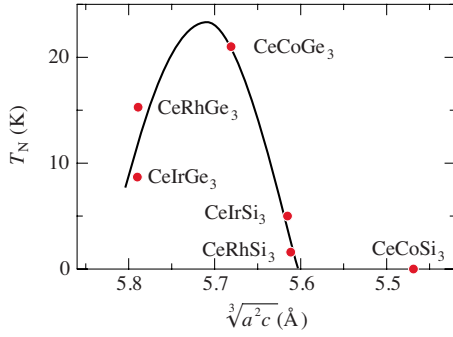


FIG. 3. (Color online) Neel temperature with respect to the averaged interatomic distance, $\sqrt[3]{a^2c}$, in noncentrosymmetric CeTX_3 compounds. This plot is related to Doniach's phase diagram (see text). Cited from Ref. 13.

AFM phase still exists. The phase diagrams of CeIrGe_3 and the other four CeTX_3 superconductors are alike, all resembling Doniach's phase diagram¹⁷ with the maximum T_N around ambient pressure and $|J|D(E_F)$ replaced by pressure. Here, $|J|$ is the magnitude of the magnetic exchange interaction and $D(E_F)$ is the density of states at the Fermi energy. This is in agreement with the discussion given above for the temperature dependence of the resistivity as a function of pressure since Doniach model assumes a competition between the RKKY interaction, responsible for localization of Ce 4*f* electrons and magnetic ordering at low pressures, and the Kondo effect, that causes itinerancy in these electrons at high pressures. Doniach model, however, predicts a Fermi-liquid phase above the QCP pressure, whereas the CeTX_3 compounds show non-Fermi-liquid behaviors.²

The exchange interaction J is also enhanced by the unit-cell volume contraction and a plot of Néel temperature versus average interatomic distance $\sqrt[3]{a^2c}$ should be in close relation with Doniach's phase diagram. This is the case shown in Fig. 3 for the CeTX_3 materials, where the QCP is located around a molar volume of 176 \AA^3 .¹³ The figure indicates that whereas, for example, in CeIrSi_3 and CeRhSi_3 the QCP appears at relatively low pressures and in CeIrGe_3 it should emerge at much higher pressure. This is confirmed by the present experiment.

We now discuss the low-temperature resistivity data of CeIrGe_3 under magnetic fields applied along the [001] direction at 24 GPa shown in Fig. 4. The high level of noise was caused by the very low bias current used to avoid both heating the sample and destroying the superconducting state. Zero resistivity was observed only under these conditions. With increasing magnetic field the onset of the resistivity drop shifts to lower temperatures, providing further evidence that such a drop is due to superconductivity. Using this onset we deduce the H_{c2}^{\parallel} plotted as a function of temperature in Fig. 5. The uncertainty in the onset temperatures was estimated to be about 120 mK. It is unknown at this point whether or not the $H_{c2}^{\parallel}(T)$ of CeIrGe_3 will develop a concave curvature at lower temperatures and/or at higher pressures near the optimum, as occurs in CeIrSi_3 , CeRhSi_3 , and CeCoGe_3 .^{8,9} Nevertheless, it is already clear from the data taken at 24 GPa (Fig. 5) that $H_{c2}^{\parallel}(0) > 10 \text{ T}$ and that it is significantly larger than the weak-coupling paramagnetic limiting field $H_p \approx 3 \text{ T}$.

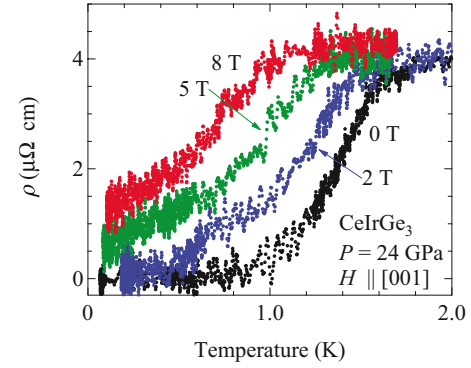


FIG. 4. (Color online) Temperature dependence of the electrical resistivity in CeIrGe_3 at different magnetic fields applied along the [001] direction.

$H_{c2}^{\parallel}(0) > H_p$ has been found in all noncentrosymmetric superconductors that emerge in the presence of an AFM phase and have a large antisymmetric spin-orbit coupling; that is, in CeIrSi_3 , CeRhSi_3 , CeCoGe_3 , CePt_3Si , and now CeIrGe_3 . It is believed that the absence of the spin paramagnetic limit is a common feature of these compounds and thus that their superconductivity is limited by orbital effects. In CeIrGe_3 the initial slope of the H_{c2}^{\parallel} vs T curve has the value $(-dH_{c2}^{\parallel}/dT)_{T_c} = 16 \text{ T/K}$. The zero-temperature orbital upper critical field $H_{c2}^{\text{orb}}(0)$ can be obtained from the formula¹⁸

$$H_{c2}^{\text{orb}}(0) = h_0 [(-dH_{c2}^{\parallel}/dT)_{T_c}] T_c. \quad (1)$$

The value h_0 depends on both the ratio ξ_0/l and the coupling parameter λ . In CeIrSi_3 , CeRhSi_3 , and CeCoGe_3 , $H_{c2}^{\parallel}(0)$ is close to the strong-coupling limit of the orbital critical field H_{c2}^{orb} . In the clean approximation the orbital-limited $H_{c2}^{\parallel}(0)$ of CeIrGe_3 should have a value between 17 T (weak coupling) and 37 T (strong coupling). From this $11 < H_{c2}^{\parallel}(0)/T_c < 25$, a large ratio only seen in noncentrosymmetric CeTX_3 materials with an AFM phase. We argue here that even though the

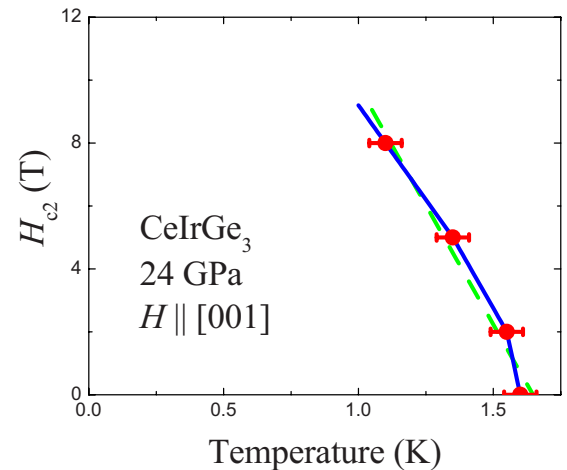


FIG. 5. (Color online) Temperature dependence of the upper critical field of CeIrGe_3 at 24 GPa. The solid line is a guide to the eye and the dashed line suggests that within experimental error the data may follow a linear behavior near T_c .

present data already suggest a very high $H_{c2}^{\parallel}(0)$ in CeIrGe₃, in noncentrosymmetric CeTX₃ superconductors the highest $H_{c2}^{\parallel}(0)$ and a concave curvature of $H_{c2}^{\parallel}(T)$ are found at pressures very close to the optimum for superconductivity. It is possible that we did not reach the optimal pressure for CeIrGe₃.

In summary, we reported on the temperature dependence of the electrical resistivity of CeIrGe₃ under high pressures up to 24 GPa. Pressure-induced superconductivity was found at 20 GPa. A significantly large upper critical field $H_{c2}(0) > 10$ T is observed, implying a large H_{c2}^{\parallel}/T_c as in the other noncentrosymmetric CeTX₃ superconductors that emerge in an AFM phase.

This work was supported by Grant-in-Aid for Scientific Research on Specially Promoted Research (Grant No. 20001004), Osaka University; Global COE Program “Core Research and Engineering of Advanced Materials-Interdisciplinary Education Center for Materials Science” (Grant No. G10); Grant-in-Aid for Scientific Research on Innovative Areas “Heavy Electrons” (Grants No. 20102002 and No. 21102511); Scientific Research under Grants No. (S)(19104009), No. (B)(21340102), and No. (B)(21740256) from the Ministry of Education, Culture, Sports, Science and Technology, Japan; and the Sasagawa Scientific Research (Grant No. 21-231) from the Japan Science Society.

-
- ¹Y. Ōnuki, R. Settai, K. Sugiyama, T. Takeuchi, T. C. Kobayashi, Y. Haga, and E. Yamamoto, *J. Phys. Soc. Jpn.* **73**, 769 (2004).
²C. Pfleiderer, *Rev. Mod. Phys.* **81**, 1551 (2009).
³I. Sugitani, Y. Okuda, H. Shishido, T. Yamada, A. Thamizhavel, E. Yamamoto, T. D. Matsuda, Y. Haga, T. Takeuchi, R. Settai, and Y. Ōnuki, *J. Phys. Soc. Jpn.* **75**, 043703 (2006).
⁴N. Kimura, K. Ito, K. Saitoh, Y. Umeda, H. Aoki, and T. Terashima, *Phys. Rev. Lett.* **95**, 247004 (2005).
⁵R. Settai, Y. Okuda, I. Sugitani, Y. Ōnuki, T. D. Matsuda, Y. Haga, and H. Harima, *Int. J. Mod. Phys. B* **21**, 3238 (2007).
⁶G. Knebel, D. Aoki, G. Lapertot, B. Salce, J. Flouquet, T. Kawai, H. Muranaka, R. Settai, and Y. Ōnuki, *J. Phys. Soc. Jpn.* **78**, 074714 (2009).
⁷M. Sigrist, D. F. Agterberg, P. A. Frigeri, N. Hayashi, R. P. Kaur, A. Koga, I. Milat, and K. Wakabayashi, *Effective Models for Low-dimensional Strongly Correlated Systems*, AIP Conf. Proc. No. 816 (AIP, New York, 2006), p. 124.
⁸N. Kimura, K. Ito, H. Aoki, S. Uji, and T. Terashima, *Phys. Rev. Lett.* **98**, 197001 (2007).
⁹M.-A. Méasson, H. Muranaka, T. Kawai, Y. Ota, K. Sugiyama, M. Hagiwara, K. Kindo, T. Takeuchi, K. Shimizu, F. Honda, R. Settai, and Y. Ōnuki, *J. Phys. Soc. Jpn.* **78**, 124713 (2009).
¹⁰M. Nakashima, K. Tabata, A. Thamizhavel, T. C. Kobayashi, M. Hedo, Y. Uwatoko, K. Shimizu, R. Settai, and Y. Ōnuki, *J. Phys.: Condens. Matter* **16**, L255 (2004).
¹¹Y. Muro, D. Eom, N. Takeda, and M. Ishikawa, *J. Phys. Soc. Jpn.* **67**, 3601 (1998).
¹²Y. Okuda, I. Sugitani, H. Shishido, T. Yamada, A. Thamizhavel, E. Yamamoto, T. D. Matsuda, Y. Haga, T. Takeuchi, R. Settai, and Y. Ōnuki, *J. Magn. Magn. Mater.* **310**, 563 (2007).
¹³T. Kawai, H. Muranaka, M.-A. Measson, T. Shimoda, Y. Doi, T. D. Matsuda, Y. Haga, G. Knebel, G. Lapertot, D. Aoki, J. Flouquet, T. Takeuchi, R. Settai, and Y. Ōnuki, *J. Phys. Soc. Jpn.* **77**, 064716 (2008).
¹⁴D. Jaccard, J. M. Mignot, B. Bellarbi, A. Benoit, H. F. Braun, and J. Sierro, *J. Magn. Magn. Mater.* **47-48**, 23 (1985).
¹⁵D. Jaccard, K. Behnia, and J. Sierro, *Phys. Lett. A* **163**, 475 (1992).
¹⁶H. Okada, K. Igawa, H. Takahashi, Y. Kamihara, M. Hirano, H. Hosono, K. Matsubayashi, and Y. Uwatoko, *J. Phys. Soc. Jpn.* **77**, 113712 (2008).
¹⁷S. Doniach, in *Valence Instabilities and Related Narrow Band Phenomena*, edited by R. D. Parks (Plenum, New York, 1977), p. 169.
¹⁸E. Helfand and N. R. Werthamer, *Phys. Rev.* **147**, 288 (1966).